

# Economically viable synthesis of Fe<sub>3</sub>O<sub>4</sub> nanoparticles and their characterization

V. Srivastava<sup>1</sup>, P.K. Singh<sup>2</sup>, C.H. Weng<sup>3</sup>, Y.C. Sharma<sup>1\*</sup>

<sup>1</sup>Department of Applied Chemistry, Institute of Technology, Banaras Hindu University Varanasi 221 005, India

<sup>2</sup>Department of Civil Engineering, Institute of Technology, Banaras Hindu University Varanasi 221 005, India

<sup>3</sup>Department of Civil and Ecological Engineering, Da-Hsu Hsiang, Kaohsiung County 84008, Taiwan

\*Corresponding author: e-mail: ysharma.apc@itbhu.ac.in

Nano iron oxide particles (Fe<sub>3</sub>O<sub>4</sub>) were synthesized by coprecipitation of Fe<sup>2+</sup> and Fe<sup>3+</sup> by ammonia solution in the aqueous phase. Various instrumentation methods such as X ray Diffractometry (XRD), Transmission Electron Microscopy (TEM), Fourier Transform Infrared (FTIR) spectroscopy, Brunauer-Emmett-Teller (BET) and Vibrating Sample Magnetometry (VSM) were used to characterize the properties of nanoparticles. The size of the nanoparticles was measured and was found to be between 10 to 15 nm. The value of saturation magnetization of the nanoparticles was found to be 55.26 emu/g. The BET surface area of nano iron oxide particles measured to be 86.55 m<sup>2</sup>/g.

**Keywords:** Nano iron, synthesis, coprecipitation, characterization, pH<sub>zpc</sub>.

## INTRODUCTION

Nano iron oxide particles (Fe<sub>3</sub>O<sub>4</sub>) have attracted attention of researchers due to their unique magnetic properties and widespread application in different fields such as magnetic storage devices, catalysis, magnetic refrigeration systems, mineral separation, heat transfer applications in drug delivery system, cancer therapy, and magnetic cell separation<sup>1-3</sup>. Application of magnetic nanoparticles in the field of wastewater treatment has also come up as an interesting area of research. Fe<sub>3</sub>O<sub>4</sub> particles possess high surface area and can easily be synthesized. Because of these properties, they have been found to be effective in removing metallic ions from wastewaters. Numerous studies have demonstrated that bulk iron oxides have good efficiency to remove heavy metals from aqueous solutions. But due to high surface area, nanosized particles have better efficiency than bulk particles of same materials<sup>4</sup>. In spite of being non-corrosive, nano iron oxide particles can be easily recovered by an external magnetic field. At nanoscale, the particles show distinct magnetic and electrical properties due to reduced size and high surface area to volume ratio<sup>5</sup>. Various methods developed to synthesize magnetic nanoparticles include co-precipitation, hydrothermal synthesis, microemulsion, pyrolysis, electrothermal synthesis, sol-gel method, mechano-chemical processing, DC thermal arc plasma method and non-aqueous route<sup>6-10</sup>. For the synthesis of Fe<sub>3</sub>O<sub>4</sub> nanoparticles, the co-precipitation of Ferrous and Ferric ion of ratio 1 to 2 in alkaline medium is the most commonly used method. In the present studies the nanoparticles have been synthesized by the coprecipitation method. The nanoparticles of iron oxide were then characterized by X-ray diffraction (XRD), transmission electron microscopy (TEM), Fourier transform infrared (FTIR), Brunauer-Emmett-Teller (BET) and the vibrating sample magnetometer (VSM).

## EXPERIMENTAL

### Synthesis of nano particles

All the chemicals used were of analytical (AR) grade. The chemicals used in this study were ferrous chloride, ferric chloride, ammonia solution, acetone, and hydrochloric acid. Ferric chloride and ferrous chloride were mixed in 2:1 molar ratio. The solutions of Fe<sup>2+</sup> and Fe<sup>3+</sup> were prepared by making their aqueous solutions in distilled water and this solution containing both ions was then heated up to 40°C for 10 min. After heating, the solution was precipitated by ammonia solution with continuous stirring on the magnetic stirrer at 40°C. Black colored particles of iron oxide were precipitated. These particles were then separated from the solution by using a strong magnet and then were washed many times with distilled water followed by washing with dilute HCl to remove the excess of OH<sup>-</sup> groups. Finally these particles were washed by acetone and then dried overnight in a hot air oven at 60°C. The synthesized nano particles were characterized by XRD, FTIR and TEM.

## RESULTS AND DISCUSSION

### Characterization of the nano particles

After drying, iron oxide particles were characterized by sophisticated methods. Phase characterization of the powder was conducted by XRD technique (X-ray diffractometer Scifert and Co. Model ID- 3000) using CuK $\alpha$  radiation, and at 2 $\theta$  = 20–80°. Crystallite size was determined by using the diffraction peaks from Scherer formula<sup>11</sup>:

$$D = K\lambda/b\cos\theta \quad (1)$$

where D is crystallite size (nm),  $\lambda$  is wavelength of the monochromatic X-ray beam (0.154056 nm for CuK $\alpha$  radiation), b is full width at half maximum for the diffraction peak under consideration (rad), K is constant (0.9),  $\theta$  is diffraction angle (degree). For accurate determination of lattice parameters, a database Powder Diffraction File JCPDS PDF release 1997, International Centre for Dif-

fraction Data (ICCD) was used. The size of the particles was also confirmed by TEM. The FTIR spectra of  $\text{Fe}_3\text{O}_4$  were obtained by using the FTIR spectrometer (Shimadzu 8400S, Japan). The sample was ground with 200 mg of KBr in a mortar and pressed in to 10 mm diameter disks under 10 tones of pressure and high vacuum. Determination of  $\text{pH}_{\text{zpc}}$  was done to investigate the surface behaviour of nano iron oxide particles<sup>12</sup>. For its determination 0.01 M NaCl was prepared and its pH was adjusted in the range between 2 to 12 by using 1 M NaOH and/or HCl. Then 50 ml of 0.01 M NaCl was taken in conical flasks and then 0.20 g of nano iron oxide powder was added to this. These flasks were then kept for 48 h and after that final pH of the solutions was measured by using the pH meter (IKON digital pH meter). Graphs were then plotted between  $\text{pH}_{\text{final}}$  vs  $\text{pH}_{\text{initial}}$ . The  $\text{pH}_{\text{zpc}}$  of the sample was recorded as the point where the curve  $\text{pH}_{\text{final}}$  vs.  $\text{pH}_{\text{initial}}$  crosses the line  $\text{pH}_{\text{initial}} = \text{pH}_{\text{final}}$ .

BET surface area, pore volumes, and pore size distribution of the sample were investigated by using a computer controlled automated porosimeter (Micromeritics ASAP 2020, V302G single port). Nitrogen was used as the cold bath (77 K) and a classical adsorption model BET theory was used for the determination of the surface area<sup>13</sup>. The porous structural parameters used in this work were taken from the BJH data. For this, the powder was evacuated under vacuum and then cooled to  $-196^\circ\text{C}$  using liquid nitrogen. The adsorption portion of the  $\text{N}_2$  isotherm was used to calculate the pore size distribution of nano iron oxide particles. To investigate the magnetic properties the hysteresis of magnetization was obtained by changing H between +5000 G and -5000 G at room temperature.

XRD measurement was conducted to identify the nanomaterial prepared with ferrous and ferric salts. The XRD of the sample (Fig. 1) shows the formation of  $\text{Fe}_3\text{O}_4$ . The formation of  $\text{Fe}_3\text{O}_4$  was indicated for synthesized nanomaterials based on the comparison of their XRD patterns with the standard pattern of  $\text{Fe}_3\text{O}_4$  (JCPDS 19-629). hkl values are known to be *Miller indices* and these are related to the crystal structure of the substance. Miller indices are the labels used to distinguish one set of parallel planes from another. It is a set of three numbers  $h k l$  that defines a set of parallel planes in a crystal. The orientation of the planes and inter-planer spacing is determined by hkl-indices values and the hkl values for different characteristic peaks for  $\text{Fe}_3\text{O}_4$  was found to be 111, 220, 311, 400, 422, 511, 440 533 and 642, respec-

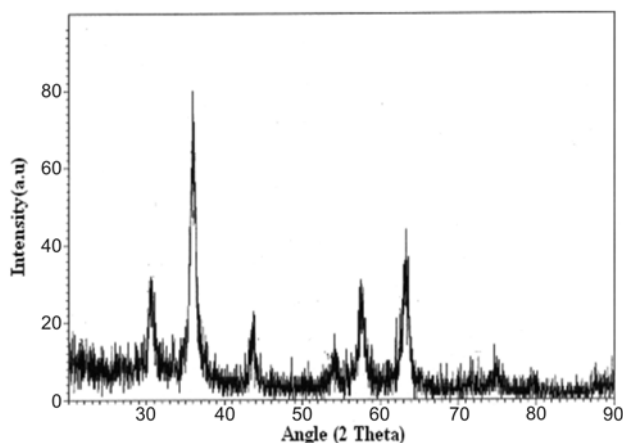


Figure 1. XRD of nano iron oxide powder

tively. The peak positions of the plane matched consistently with those of the standard data for magnetite demonstrating that the synthesized black powders were magnetite particles. In addition of the peaks of  $\text{Fe}_3\text{O}_4$  some peaks of  $\gamma\text{-Fe}_2\text{O}_3$  were also found in the prepared powder. The application of Scherrer's formula to the (311) reflection peak indicated the formation of  $\text{Fe}_3\text{O}_4$  nanoparticles with approximately 15 nm in diameter. The main peaks of  $\text{Fe}_3\text{O}_4$  in the XRD pattern are broadened, indicating the crystalline sizes of the  $\text{Fe}_3\text{O}_4$  nanoparticles are very small. Further, the TEM (Figs. 2a and 2b) of the nano iron oxide confirms nanosize of prepared powder. The figures also indicate the formation of fine particles.

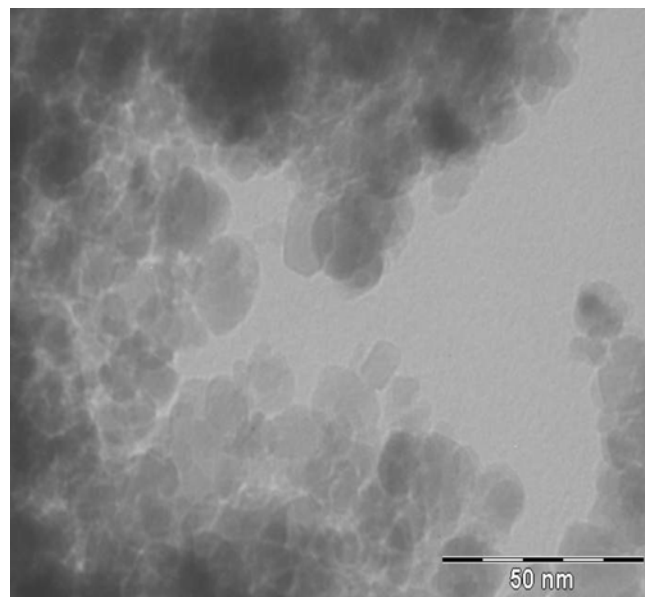


Figure 2a. TEM of nano iron oxide particles

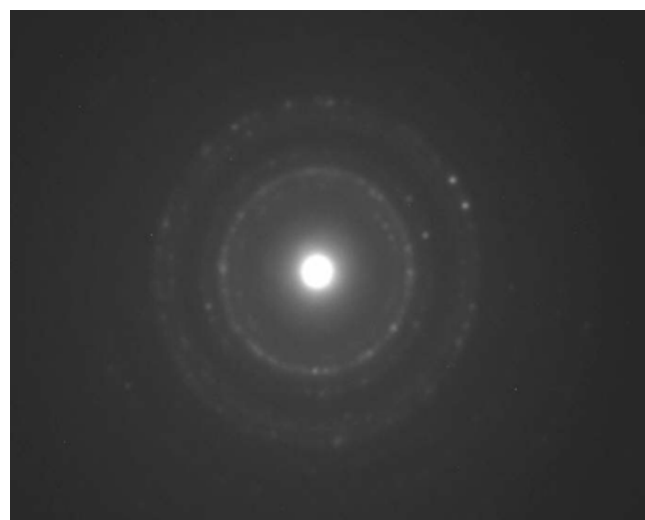


Figure 2b. SADP(selected area diffraction pattern) of nano Iron oxide particles

The FTIR spectroscopy was also used to characterize the synthesized magnetite. Fig. 3 depicts the FTIR of synthesized nano iron oxide particles. The presence of the peaks in the region  $3000\text{--}3500\text{ cm}^{-1}$  are related with the lattice of water molecules. It indicates the presence of moisture in the powder or KBr. Peak at near about  $570\text{ cm}^{-1}$  is due to metal oxygen (Fe-O) functional groups. The broad bands around  $570\text{ cm}^{-1}$  correspond to stretching vibrations of Fe -O bonds typical of the crystalline lattice

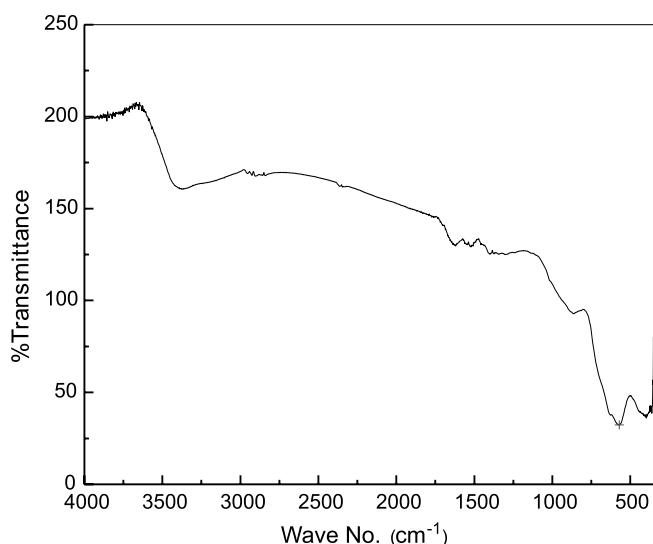


Figure 3. FTIR of magnetic nano iron oxide particles

of magnetite. This peak is very sharp and of strong intensity indicating crystallinity of the sample.

$pH_{zpc}$  plays an important role in characterizing the nature of the surface of any adsorbent and the removal of adsorbates strongly depends upon  $pH_{zpc}$  of surface of the adsorbent. The graph for the determination of  $pH_{zpc}$  of nano iron oxide is shown in Fig. 4. The  $pH_{zpc}$  of the sample was found to be 7.1. Similar findings were also reported in some of the previous studies<sup>13</sup>.

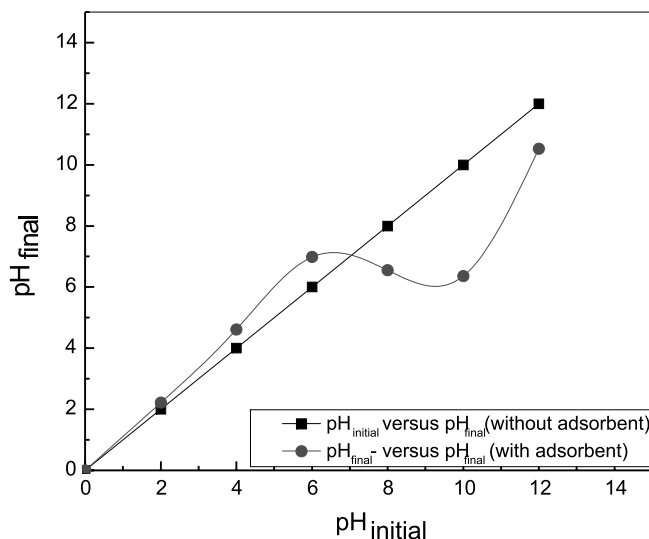


Figure 4. The plot for the determination of  $pH_{zpc}$  of nano iron oxide

Figures 5a, 5b, and 5c show the  $N_2$  gas adsorption-desorption isotherms, cumulative pore volume and BET pore size distribution respectively of the magnetic nano iron oxide particles. The data obtained by Brunauer-Emmett-Teller (BET) measurements are shown in tabular form in Table 1. BET surface area of prepared nano powder was measured and found to be  $86.55 \text{ m}^2/\text{g}$ .

Fig. 6. shows the hysteresis loops measured at room temperature for nano iron oxide particles. The saturation magnetization ( $M_s$ ) value of the sample measured as  $55.26 \text{ emu/g}$  at room temperature. The value of the saturation magnetization is comparatively lower than that of bulk magnetite which is  $93 \text{ emu/g}$ <sup>15-17</sup>. Smaller the particle

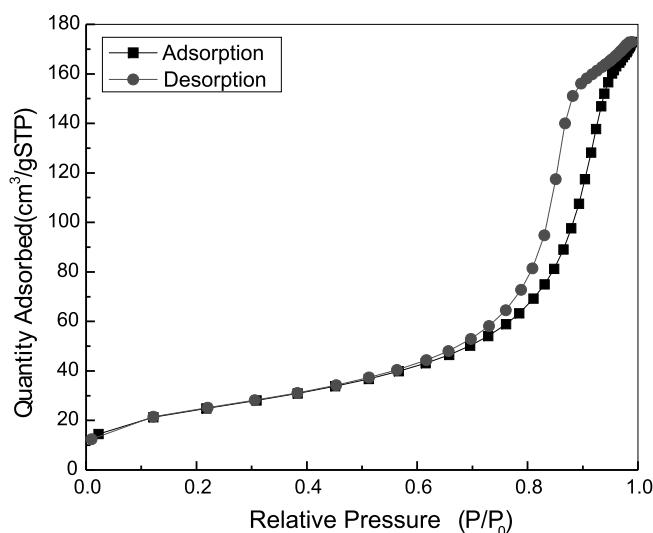


Figure 5a. The  $N_2$  gas adsorption-desorption isotherm for the magnetic nano iron oxide particles

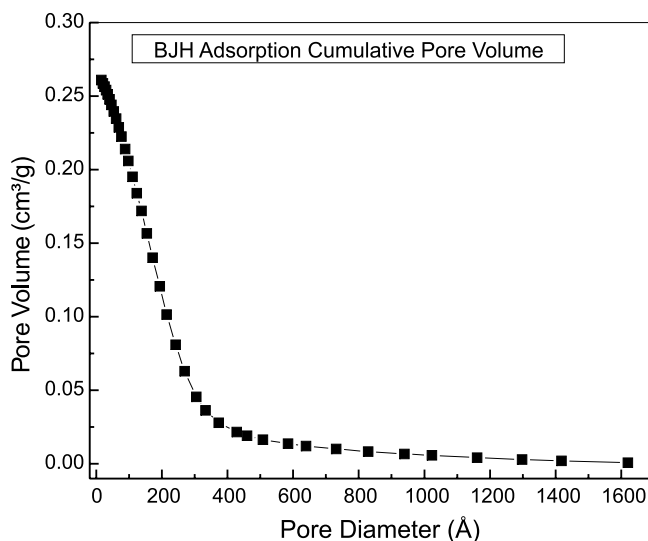


Figure 5b. The cumulative pore volume of magnetic nano iron oxide particles

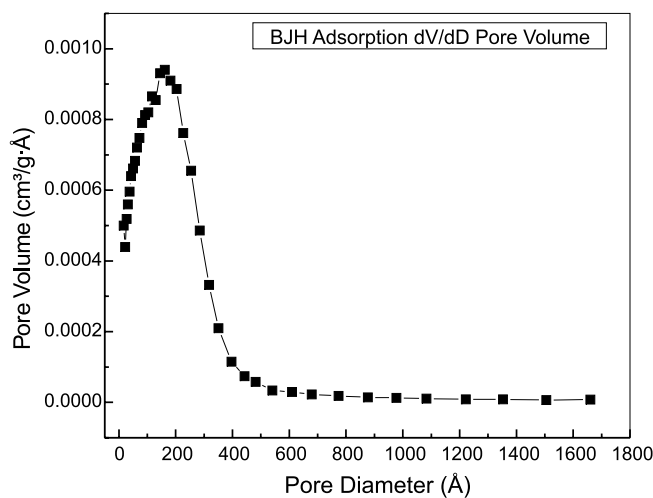
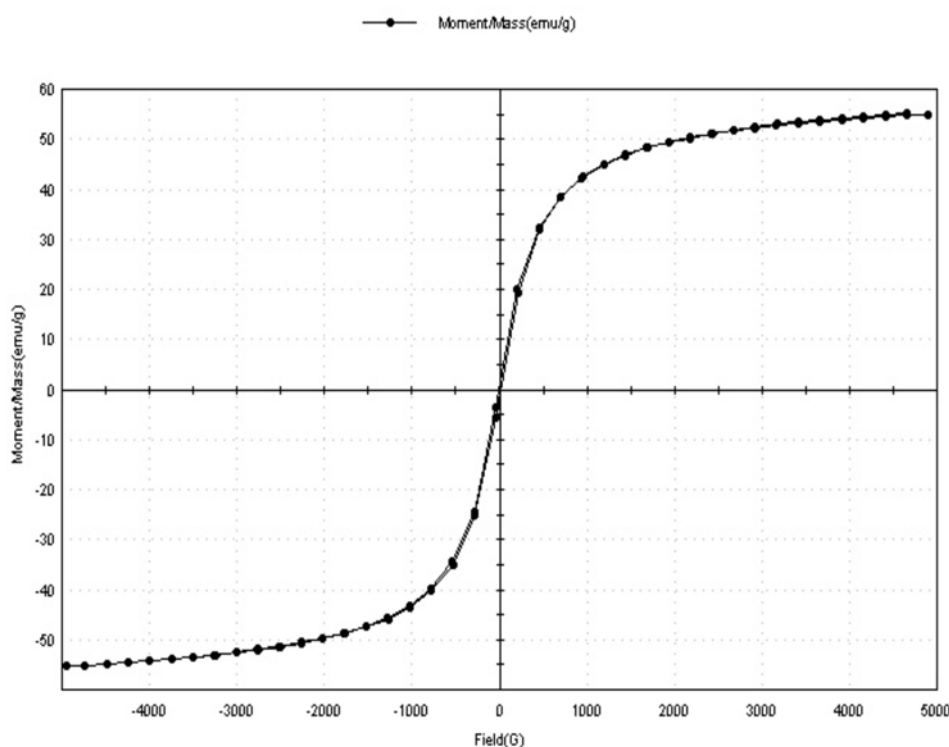


Figure 5c. BET pore size distribution for the magnetic nano iron oxide particles

size, the larger is the part of atoms present in the surface layer where the crystal structure is disordered preventing magnetism. Therefore, the smaller particles apparently have lower value of magnetization saturation. The value of remanence ( $M_r$ ) and coercive force was found to be  $1.204 \text{ emu/g}$  and  $12.191 \text{ G}$ , respectively.

**Table 1.** The results of Brunauer-Emmett-Teller (BET) measurements

Surface Area	BET surface area (m <sup>2</sup> /g)	86.55
	BJH adsorption cumulative surface area of pores (m <sup>2</sup> /g)	86.65
	BJH desorption cumulative surface area of pores (m <sup>2</sup> /g)	91.14
Pore volume	Single point adsorption total pore volume of pores (cm <sup>3</sup> /g)	0.27
	BJH adsorption cumulative volume of pores (cm <sup>3</sup> /g)	0.26
	BJH desorption cumulative volume of pores (cm <sup>3</sup> /g)	0.26
Pore size	Adsorption average pore width (Å)	123.59
	BJH adsorption average pore diameter (Å)	120.48
	BJH desorption average pore diameter (Å)	113.75

**Figure 6.** The hysteresis loop of the synthesized Fe<sub>3</sub>O<sub>4</sub> nanoparticles at room temperature

### Summary

The work reported is novel and the novelty of study lies in the fact that the material has been synthesized by economically viable methods. Precursors, which have been used for synthesis of nanomaterial is not very costly. As different available techniques of preparation of nanomaterial required expensive instruments resulting in the escalated cost of the preparation of the material, but we have used a very simple and non expensive setup for synthesizing the nano iron oxide. This technique is not only cost effective but it also gives high purity product and greater yield in a very short duration. Surface area of synthesised nanomaterial was significant which further confirms its applicability in different application such as for water treatment by adsorption technique.

### CONCLUSIONS

On the basis of the present studies, the following conclusion may be drawn:

- The process of preparation of Fe<sub>3</sub>O<sub>4</sub> is cost effective because of the use of inexpensive precursors.
- Fe<sub>3</sub>O<sub>4</sub> particles can be prepared at low temperature.
- Almost all the particles are uniform in shape. XRD and TEM confirm phase and its nanosize.

– The value of saturation magnetization was recorded to be 55.26 emu/g.

– The synthesized nano iron oxide particles were found to be of significant value of BET surface area so it can be successfully used in the adsorption technique for removing the pollutant species from wastewater.

### Acknowledgements

The authors are thankful to AICTE, Government of India, for providing financial assistance in form of RPS (Scheme No 10313).

### LITERATURE CITED

1. Liu, Z.L., Wang, H.B., Lu, Q.H., Du, G.H., Peng, L., Du, Y.Q., Zhang, S.M. & Yao, K.L. (2004). Synthesis and characterization of ultra fine well dispersed magnetic nanoparticles. *J. Magnetism Magnetic Mater.* 283, 258–262. DOI:10.1016/j.jmmm.2004.05.031.
2. Salazar, J.S., Roman, M.A.C. & Gomez, L.B. (2007). Structural and magnetic domains characterization of magnetic nanoparticles. *Mater. Sci. Eng. C.* 27, 317–320. DOI:10.1016/j.msec.2006.07.027.
3. Thapa, D., Palkar, V.R., Kurup, M.B. & Malik, S.K. (2004). Properties of magnetic nano particles synthesized through a novel chemical route. *Mater. Lett.* 58, 2692–2694. DOI:10.1016/j.matlet.2004.03.045.

4. Sharma, Y.C., Srivastava, V., Singh, V.K., Kaul, S.N. & Weng, C.H. (2009). Nanoadsorbents for the removal of metallic pollutants from water and wastewater. *Environ. Technol.* 30, 583–609. DOI :10.1080/09593330902838080.
5. Ozkaya, T., Toprak, M.S., Baykal, A., Kavas, H., Koseoglu, Y. & Aktas, B. (2009). Synthesis of Fe<sub>2</sub>O<sub>3</sub> nanoparticles at 100 °C and its magnetic characterization. *J. Alloy. Comp.*, 472, 18–23. DOI:10.1016/j.jallcom.2008.04.101.
6. Sharma, Y.C., Srivastava, V., Upadhyay, S.N. & Weng, C.H. (2008). Aluminum nanoparticles for the removal of Ni(II) from aqueous solutions. *Ind. Eng. Chem. Res.*, 47, 8095–8100. DOI: 10.1021/ie800831v.
7. Swihart, M.T. (2003). Vapor phase synthesis of nanoparticles. *Curr. Opin. Colloid Interf. Sci.* 8, 127–133. DOI:10.1016/S1359-0294(03)00007-4.
8. Feng, N.S., Yang, L., Hua, X. & Hua, L.Z. (2005). Removal of hexavalent chromium from aqueous solutions by iron nanoparticles. *J. Zhejiang Univ. Sci.* 6B, 1022–1027. DOI: 10.1007/BF02888495.
9. Murray, C.B., Kagan, C.R. & Bawendi, M.G. (2000). Synthesis and characterization of monodisperse nano crystals and close packed assemblies. *Annu. Rev. Mater. Sci.* 30, 545–610. DOI: 10.1146/annurev.matsci.30.1.545.
10. Hann, H. (1997). Gas phase synthesis of nanocrystalline materials. *Nanostruct. Mater.* 9, 3–12. PII 80965-9773(97)00013-5.
11. Biasi, R.S.D., Figueiredo, A.B.S., Fernandes, A.A.S. & Larica, C. (2007). Synthesis of cobalt ferrite nanoparticles using combustion waves. *Solid State Commun.* 144, 15–17. DOI:10.1016/j.ssc.2007.07.031.
12. Nomanbhay, M. & Palanisamy, K. (2005). Removal of heavy metal from industrial wastewater using chitosan coated oil palm shell charcoal. *Electronic J Biotechnol.* 8, 43–53.
13. Sun, Y., Zhang, J.P., Yang, G. & Li, Z.H. (2007). Preparation of activated carbon with large specific surface area from reed black liquor. *Environ. Technol.* 28, 491–497. DOI: 10.1080/09593332808618810.
14. Kanel, S.R., Charlet, B. & Choi, L. (2005). Removal of As(III) from ground water by nanoscale zerovalent iron. *Environ. Sci. Technol.* 39, 1291–1298. DOI: 10.1021/es048991u.
15. Verges, M.A., Costo, R., Roca, A.G., Marco, J.F., Goya, G.F., Serna, C.J. & Morales, M.P. (2008). Uniform and water stable magnetic nanoparticles with diameters around the monodomain-multidomain limit. *J. Phys. D: Appl. Phys.* 41, 134003–134013. DOI: 10.1088/0022-3727/41/13/134003.
16. Qi, B., Li, D., Ni & Zheng, H. (2007). A facile reduction route to the preparation of single-crystalline iron nanocubes, *Chem. Lett.* 36, 722–723. DOI:10.1246/cl.2007.722.
17. Iida, H., Takayanagi, K., Nakanishi, T. & Osaka, T. (2007). Synthesis of Fe<sub>3</sub>O<sub>4</sub> nanoparticles with various sizes and magnetic properties by controlled hydrolysis. *J. Colloid Interf. Sci.* 314, 274–280. DOI:10.1016/j.jcis.2007.05.047.